





## RESEARCH ARTICLE

## CPEB4–CLOCK crosstalk during temporal lobe epilepsy

Laura de Diego-Garcia<sup>1,2</sup>  | Gary P. Brennan<sup>3,4</sup> | Theresa Auer<sup>3</sup> |  
 Aida Menendez-Mendez<sup>1</sup> | Alberto Parras<sup>1,5</sup> | Alba Martin-Gil<sup>2</sup> | Meghma Mitra<sup>1</sup> |  
 Ivana Ollà<sup>5,6</sup> | Leticia Villalba-Benito<sup>3,4</sup> | Beatriz Gil<sup>1</sup> | Mariana Alves<sup>1</sup> |  
 Kelvin Lau<sup>1,4</sup> | Norman Delanty<sup>4,7,8</sup>  | Alan Beausang<sup>8</sup> | Jane Cryan<sup>8</sup> |  
 Francesca M. Brett<sup>8</sup> | Michael A. Farrell<sup>8</sup> | Donncha F. O'Brien<sup>8</sup> | Raúl Mendez<sup>9,10</sup> |  
 Gonzalo Carracedo-Rodríguez<sup>2</sup> | David C. Henshall<sup>1,4</sup>  | José J. Lucas<sup>5,6</sup> |  
 Tobias Engel<sup>1,4</sup> 

<sup>1</sup>Department of Physiology and Medical Physics, Royal College of Surgeons in Ireland, University of Medicine and Health Sciences, Dublin, Ireland, RCSI University of Medicine and Health Sciences, Dublin, Ireland

<sup>2</sup>Ocupharm Group Research, Faculty of Optics and Optometry, University Complutense of Madrid, Madrid, Spain

<sup>3</sup>School of Biomolecular and Biomedical Science, UCD Conway Institute, University College Dublin, Dublin, Ireland

<sup>4</sup>FutureNeuro, Science Foundation Ireland Research Centre for Chronic and Rare Neurological Diseases, Royal College of Surgeons in Ireland, University of Medicine and Health Sciences, Dublin, Ireland

<sup>5</sup>Center for Molecular Biology "Severo Ochoa," Spanish National Research Council/Autonomous University of Madrid, Madrid, Spain, Centro de Biología Molecular Severo Ochoa, CSIC/UAM, Madrid, Spain

<sup>6</sup>Networking Research Center on Neurodegenerative Diseases, Instituto de Salud Carlos III, Madrid, Spain

<sup>7</sup>School of Pharmacy and Biomolecular Sciences, Royal College of Surgeons in Ireland, University of Medicine and Health Sciences, Dublin, Ireland

<sup>8</sup>Beaumont Hospital, Dublin, Ireland

<sup>9</sup>Institute for Research in Biomedicine, Barcelona Institute of Science and Technology, Barcelona, Spain

<sup>10</sup>Institució Catalana de Recerca i Estudis Avançats, Barcelona, Spain

## Correspondence

Tobias Engel, Department of Physiology and Medical Physics, RCSI University of Medicine and Health Sciences, Dublin D02 YN77, Ireland.  
 Email: [tengel@rcsi.ie](mailto:tengel@rcsi.ie)

## Funding information

H2020 Marie Skłodowska-Curie Actions, Grant/Award Number: 766124 and 796600; Irish Research Council, Grant/Award Number: GOIPD/2020/806; Programa de Atracción de Talento de la Comunidad de Madrid, Grant/Award Number: 2020-T2/BMD-20180; Science Foundation Ireland, Grant/Award Number: 16/RC/3948 and 17/CDA/4708; Spanish Ministry of Economy and Competitiveness/Ministry of Science, Innovation and Universities, Grant/Award Number: PID2021-123141OB-I00

## Abstract

**Objective:** Posttranscriptional mechanisms are increasingly recognized as important contributors to the formation of hyperexcitable networks in epilepsy. Messenger RNA (mRNA) polyadenylation is a key regulatory mechanism governing protein expression by enhancing mRNA stability and translation. Previous studies have shown large-scale changes in mRNA polyadenylation in the hippocampus of mice during epilepsy development. The cytoplasmic polyadenylation element-binding protein CPEB4 was found to drive epilepsy-induced poly(A) tail changes, and mice lacking CPEB4 develop a more severe seizure and epilepsy phenotype. The mechanisms controlling CPEB4 function and the downstream pathways that influence the recurrence of spontaneous seizures in epilepsy remain poorly understood.

**Methods:** Status epilepticus was induced in wild-type and CPEB4-deficient male mice via an intra-amygdala microinjection of kainic acid. CLOCK binding to the CPEB4 promoter was analyzed via chromatin immunoprecipitation assay and melatonin levels via high-performance liquid chromatography in plasma.

**Results:** Here, we show increased binding of CLOCK to recognition sites in the CPEB4 promoter region during status epilepticus in mice and increased *Cpeb4* mRNA levels in N2A cells overexpressing CLOCK. Bioinformatic analysis of CPEB4-dependent genes undergoing changes in their poly(A) tail during epilepsy found that genes involved in the regulation of circadian rhythms are particularly enriched. *Clock* transcripts displayed a longer poly(A) tail length in the hippocampus of mice post-status epilepticus and during epilepsy. Moreover, CLOCK expression was increased in the hippocampus in mice post-status epilepticus and during epilepsy, and in resected hippocampus and cortex of patients with drug-resistant temporal lobe epilepsy. Furthermore, CPEB4 is required for CLOCK expression after status epilepticus, with lower levels in CPEB4-deficient compared to wild-type mice. Last, CPEB4-deficient mice showed altered circadian function, including altered melatonin blood levels and altered clustering of spontaneous seizures during the day.

**Significance:** Our results reveal a new positive transcriptional–translational feedback loop involving CPEB4 and CLOCK, which may contribute to the regulation of the sleep–wake cycle during epilepsy.

#### KEYWORDS

circadian rhythm, CLOCK, CPEB4, cytoplasmic polyadenylation, epilepsy, status epilepticus

## 1 | INTRODUCTION

Alterations in posttranscriptional regulatory mechanisms are widely accepted features of brain diseases including epilepsy.<sup>1–3</sup> Cytoplasmic polyadenylation is a key process by which dormant, translationally inactive messenger RNAs (mRNAs) become activated via the elongation of their poly(A) tails.<sup>4</sup> Cytoplasmic polyadenylation element-binding proteins (CPEB1–4) are sequence-specific RNA-binding proteins and key regulators of mRNA translation via the modulation of poly(A) tail length.<sup>5,6</sup> CPEBs bind to the cytoplasmic polyadenylation element, located within the 3′ untranslated region of mRNA, where, upon binding, they recruit a complex of factors that regulate poly(A) tail length, controlling both translational repression and activation.<sup>4</sup> CPEBs mediate several cellular processes in the brain pertinent to epileptogenesis, including synaptic plasticity and expression of neurotransmitter receptors,<sup>7,8</sup> and have recently been linked to several brain diseases, including autism,<sup>9</sup> Huntington disease<sup>10</sup> and epilepsy.<sup>11</sup> Supporting a role of CPEBs during the development of epilepsy, data have shown that >25% of the total transcriptome in the hippocampus undergoes alterations in their poly(A) tail after status epilepticus (SE) in mice.<sup>11</sup> Of note, CPEB4 binders were highly enriched among genes displaying an altered poly(A) tail length.<sup>11</sup> Moreover, CPEB4-deficient mice showed a more severe seizure and epilepsy phenotype following an intra-amygdala microinjection of kainic acid (KA).<sup>11</sup>

#### Key Points

- Increased binding of CLOCK to the CPEB4 promoter was seen in the hippocampus after status epilepticus
- Increased CLOCK poly(A) tail length and expression were seen in the brain post-status epilepticus and during epilepsy in mice
- Increased CLOCK and CPEB4 expression was seen in the hippocampus and cortex of TLE patients
- CPEB4-deficient mice presented lower CLOCK expression in the hippocampus and altered melatonin levels in plasma
- The CPEB4–CLOCK axis may represent an additional pathway that contributes to the regulation of the sleep–wake cycle during epilepsy

Changes in the circadian rhythm of people living with epilepsy have been proposed as both cause and consequence of the disease.<sup>12</sup> Deficiency of both CLOCK (circadian locomotor output cycles kaput) and BMAL1 (muscle Arnt-like protein 1) lowers the seizure threshold in mice, supporting a causal role for proteins regulating molecular changes during the sleep–wake cycle in epilepsy.<sup>13–15</sup> Links to mRNA polyadenylation and CPEB4 have emerged, with data showing that the circadian clock

regulates the dynamic polyadenylation status of mRNAs and that CPEB4 expression oscillates with circadian rhythmicity.<sup>16,17</sup> What regulates the circadian molecular machinery during epilepsy, and whether CPEB4 contributes to its regulation, have not been investigated to date.

Here, we show increased binding of CLOCK to the promoter of *Cpeb4* during SE and increased *Cpeb4* expression induced via CLOCK overexpression in N2A cells. In addition, we show increased CLOCK mRNA polyadenylation and expression in the brain following SE and during epilepsy, which is most likely under the control of CPEB4. Taken together, our results describe a CLOCK–CPEB4 axis as a molecular mechanism possibly contributing to the timing of spontaneous seizure recurrence in epilepsy.

## 2 | MATERIALS AND METHODS

Chemicals have been purchased from Sigma-Aldrich, Dublin, Ireland, if not stated otherwise. For Western blotting and quantitative polymerase chain reaction (qPCR) description, please refer to our extended [Supplementary Methods](#) and [Table S2](#).

### 2.1 | Animals

All animal studies adhered to the principles of the European Communities Council Directive (2010/63/EU), and relevant national licenses were approved by the Research Ethics Committee of the Royal College of Surgeons in Ireland (RCSI; REC 1322) and the Irish Products Regulatory Authority (AE19127/P038). Eight- to 12-week-old C57BL/6J male mice were sourced from the Biomedical Research Facility (RCSI) and housed in the Microsurgical Research and Training Facility (RCSI). CPEB4-deficient mice harbor a deletion of the constitutive exon 2, resulting in a premature stop codon.<sup>11,18</sup> Mice were housed in groups of 2–5/cage and kept in a controlled animal facility on a 12-h light/dark cycle at  $22 \pm 1^\circ\text{C}$ , with humidity of 40%–60%. A red light, which does not disrupt circadian rhythmicity, was present during the dark period.

### 2.2 | Mouse model of SE

Before cannula implantation, mice were anesthetized using isoflurane (5% induction, 1%–2% maintenance) and maintained normothermic by means of a feedback-controlled heat blanket (Harvard Apparatus).<sup>11</sup> Once fully anesthetized, mice were placed in a stereotaxic frame and a midline scalp incision was performed to expose

the skull. A guide cannula (anteroposterior = .94 mm, lateral = 2.85 mm) was fixed in place with dental cement. SE was induced by a microinjection of .3  $\mu\text{g}$  KA in .2  $\mu\text{L}$  phosphate-buffered saline (PBS) into the right basolateral amygdala (intra-amygdala KA [IAKA]). Vehicle-injected control animals received .2  $\mu\text{L}$  of sterile PBS. The anticonvulsant lorazepam (6 mg/kg; Wyeth) was delivered via intraperitoneal injection 40 min post-KA/vehicle.

### 2.3 | Long-term electroencephalographic monitoring

Continuous electroencephalographic (EEG) recordings were carried out using implantable EEG telemetry devices (Data Science International; model F20-EET).<sup>11</sup> Transmitters were implanted in a subcutaneous pocket, between the shoulders, and connected to four cortical EEG electrodes fixed with dental cement, one on top of each hippocampus and the reference electrodes on top of the frontal cortex. EEG data were reviewed daily, and an observer unaware of genotype manually scored seizures during the light (7:00 a.m. to 7:00 p.m.) and dark period (7:00 p.m. to 7:00 a.m.).

### 2.4 | Human brain tissue

This study was approved by the Ethics (Medical Research) Committee at Beaumont Hospital, Dublin (05/18), and written informed consent was obtained from all patients. Epilepsy patients, all diagnosed with temporal lobe epilepsy (TLE; four females and four males, average age =  $37 \pm 10.5$  years), were referred for surgical resection of the temporal lobe ([Table S1](#)). Hippocampi ( $n = 4$ ) and cortex ( $n = 4$ ) were obtained, frozen in liquid nitrogen, and stored at  $-80^\circ\text{C}$ . A pathologist confirmed the absence of significant neuronal loss. Autopsy control samples (two females and two males, average age =  $35 \pm 15.49$  years) from the temporal hippocampus ( $n = 4$ ) and cortex ( $n = 4$ ) were obtained from the Brain and Tissue Bank for Developmental Disorders at the University of Maryland, Baltimore, Maryland, USA.

### 2.5 | Blood sampling

Blood samples were collected from 8–12-week-old male *CPEB4*<sup>+/-</sup> mice and wild-type (WT) control littermates (*CPEB4*<sup>+/+</sup>) from the submandibular vein into EDTA-containing tubes at 10:00 (light cycle) and 21:00 (dark cycle). Plasma was separated from whole blood by

centrifugation (4000× g for 10 min at 4°C) and stored at −80°C until analysis of melatonin concentrations via high-performance liquid chromatography (HPLC).

## 2.6 | Cell culture and transfection

Mouse neuroblastoma 2A (N2A) cell line was maintained in Dulbecco's Modified Eagle/Nutrient Mixture F-12 medium (Invitrogen) supplemented with 10% fetal bovine serum and 100 U/mL penicillin/streptomycin. For transient transfection, N2A cells were seeded in antibiotic-free medium in 12-well plates (8×10<sup>4</sup> cells/well) and transfected (24 h later at 70% confluency) with 1 μg enhanced green fluorescent protein–CLOCK plasmid construct/well using Lipofectamine 2000 reagent (Invitrogen) according to the manufacturer's instructions. After 6 h, transfection medium was changed back to normal growth medium. Twenty-four hours after transfection, cells were washed twice in PBS and harvested in Trizol. Experiments were repeated twice.

## 2.7 | High-performance liquid chromatography

Tubes containing serum were heated at 98°C for 2 min and put on ice for an additional 10 min. To pellet proteins, tubes were then centrifuged at 15 870 g for 10 min at 4°C.<sup>19</sup> Melatonin concentrations were measured with an Agilent 1260 HPLC system (Agilent Technologies). The chromatographic system consisted of a Kromaphase C18 column with a particle size of 5 μm, a pore size of 100 Å, 25 cm in length, with .46-cm inner diameter. The system was equilibrated overnight with 40% methanol and 60% ultrapure water. Measurements were performed at a constant temperature of 20°C and a flow rate of .8 mL/min, fixing the detector at a wavelength of 244 nm. Quantification of melatonin was performed by comparing the samples with external standards.

## 2.8 | Chromatin immunoprecipitation assay

Ipsilateral hippocampi were dissected 1 h post-SE, homogenized in 1% formaldehyde, and incubated at room temperature for 10 min.<sup>20</sup> Formaldehyde was quenched with .125 mol·L<sup>−1</sup> glycine. Samples were then incubated in a hypotonic buffer (20 mmol·L<sup>−1</sup> Tris–HCl, 10 mmol·L<sup>−1</sup> NaCl, 3 mmol·L<sup>−1</sup> MgCl<sub>2</sub>), lysed in a dounce homogenizer, and rotated at 4°C for 20 min. One percent NP-40 was added to each sample, then samples were

centrifuged at 19 900 g for 5 min at 4°C and chromatin was sheared in a Diagenode sonicator. To ensure appropriate shearing profiles, DNA was analyzed on a 2% agarose gel and visualized on an ultraviolet box (VWR International). Then, samples were incubated with magnetic Dynabeads (Thermo Fisher Scientific) that had been preincubated overnight with 5 μg of CLOCK antibody (Abcam ab3517) or IgG control (Cell Signaling). Beads and DNA were incubated at 4°C for 1 h. Magnetic beads and bound material were washed with radioimmunoprecipitation assay buffer to remove loosely bound DNA/proteins. Beads were then separated from complexed DNA using Chelex reagent and heated to 100°C for 10 min. Samples were incubated at room temperature for a further 10 min before being centrifuged at 19 900 g for 5 min. The supernatant was transferred to a new tube, stored at 4°C, and quantified by qPCR with gene-specific primers. Transcription factor occupancy was normalized to IgG binding to the DNA and calculated as a percentage of total input. Primers used were as follows: *Clock*: forward: 5′-GGAAAACCCGCCTCTCCTTC-3′; reverse: 5′-GAGGCCTGCCCTGAGTAAAG-3′.

## 2.9 | Statistical analysis

For statistical analysis, we used GraphPad Prism 9. Data is presented as mean ± SEM. Analysis of variance with post hoc Fisher protected least significant difference and Tukey test was used to analyze group data of three or more. For two-group comparisons, Student *t*-test was used to determine statistical differences between groups. Significance was accepted at *p* < .05.

## 3 | RESULTS

### 3.1 | Increased occupancy of the CPEB4 promoter by CLOCK after SE

To identify possible transcriptional regulatory mechanisms governing CPEB4 expression in the brain, we analyzed the promoter region (5000 bases upstream of transcriptional start site [*GRCm39/mm39*]) of the *Cpeb4* gene for transcription factor recognition motifs. This revealed one E-box within 5000 base pairs upstream of the CPEB4 transcriptional start site. We also found, however, several further upstream, within 10 000 base pairs (Figure 1A). E-box elements are targeted by several transcription factors including *Clock*, a key regulator of circadian rhythms and previously associated with epilepsy.<sup>14,21,22</sup> We next performed a chromatin immunoprecipitation assay using a CLOCK-specific antibody in tissue from the ipsilateral

hippocampus from mice subjected to IAKA-induced SE 1 h postlorazepam. CLOCK binding to the *Cpeb4* promoter was increased by approximately threefold in mice subjected to SE (Figure 1B). Additionally, overexpression of CLOCK in N2A cells led to dramatic increases in *Cpeb4* transcript levels, further suggesting *Cpeb4* is under the transcriptional control of CLOCK (Figure 1C). In line with previous data showing increased *Cpeb4* expression in the hippocampus shortly following SE<sup>11</sup> and CLOCK activating *Cpeb4* transcription, CPEB4 protein levels were increased in mice 1 h post-SE (Figure 1D).

### 3.2 | CPEB4-mediated mRNA polyadenylation disproportionately affects genes involved in the regulation of circadian rhythms

To identify what pathways are regulated via CPEB4 post-SE and during epilepsy, we analyzed our published dataset on poly(A) tail changes occurring in the hippocampus of the IAKA mouse model (Figure 2A),<sup>11</sup> restricting our analysis, however, to previously identified CPEB4 binders.<sup>9</sup> This showed that CPEB4 binders were overrepresented

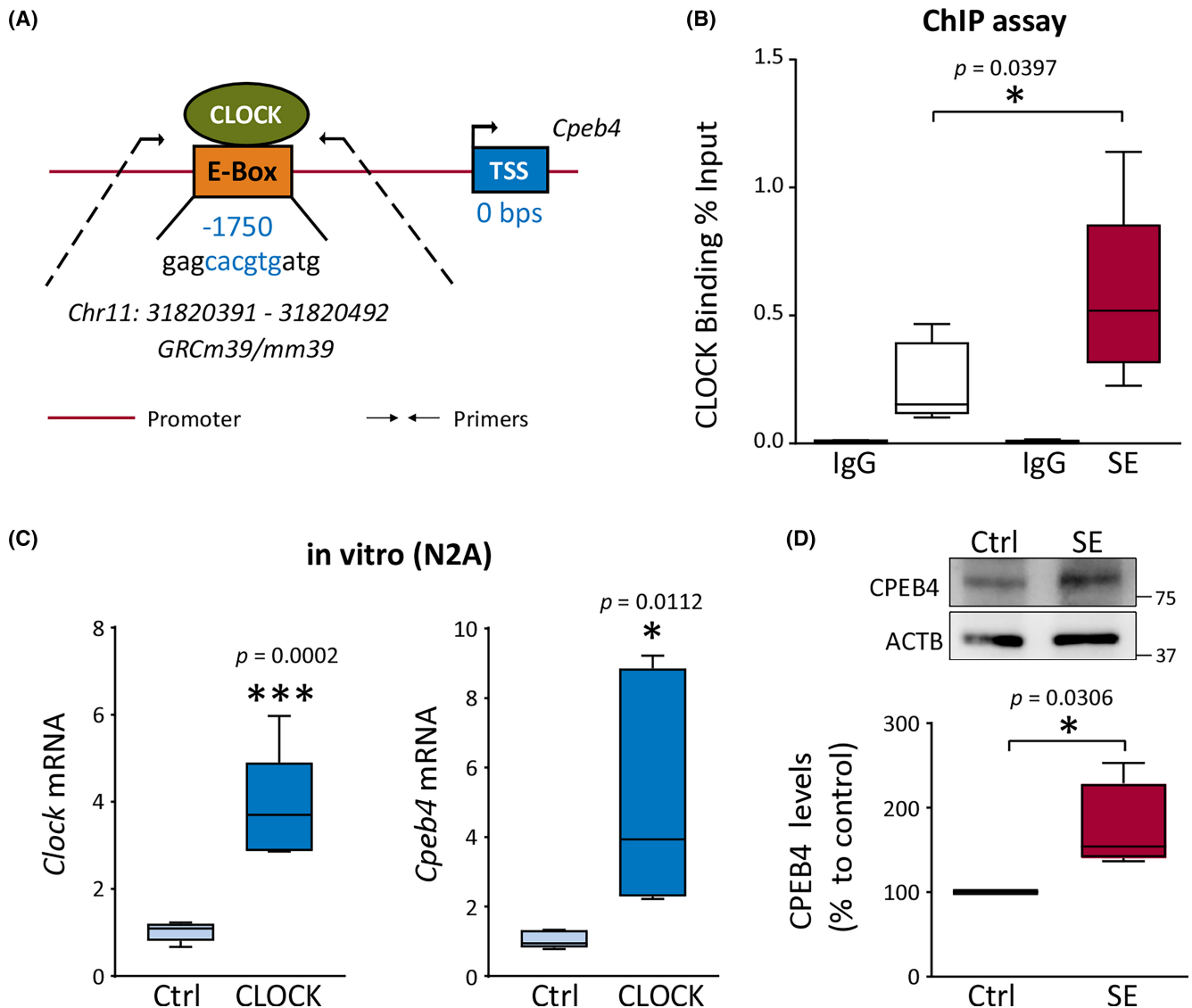
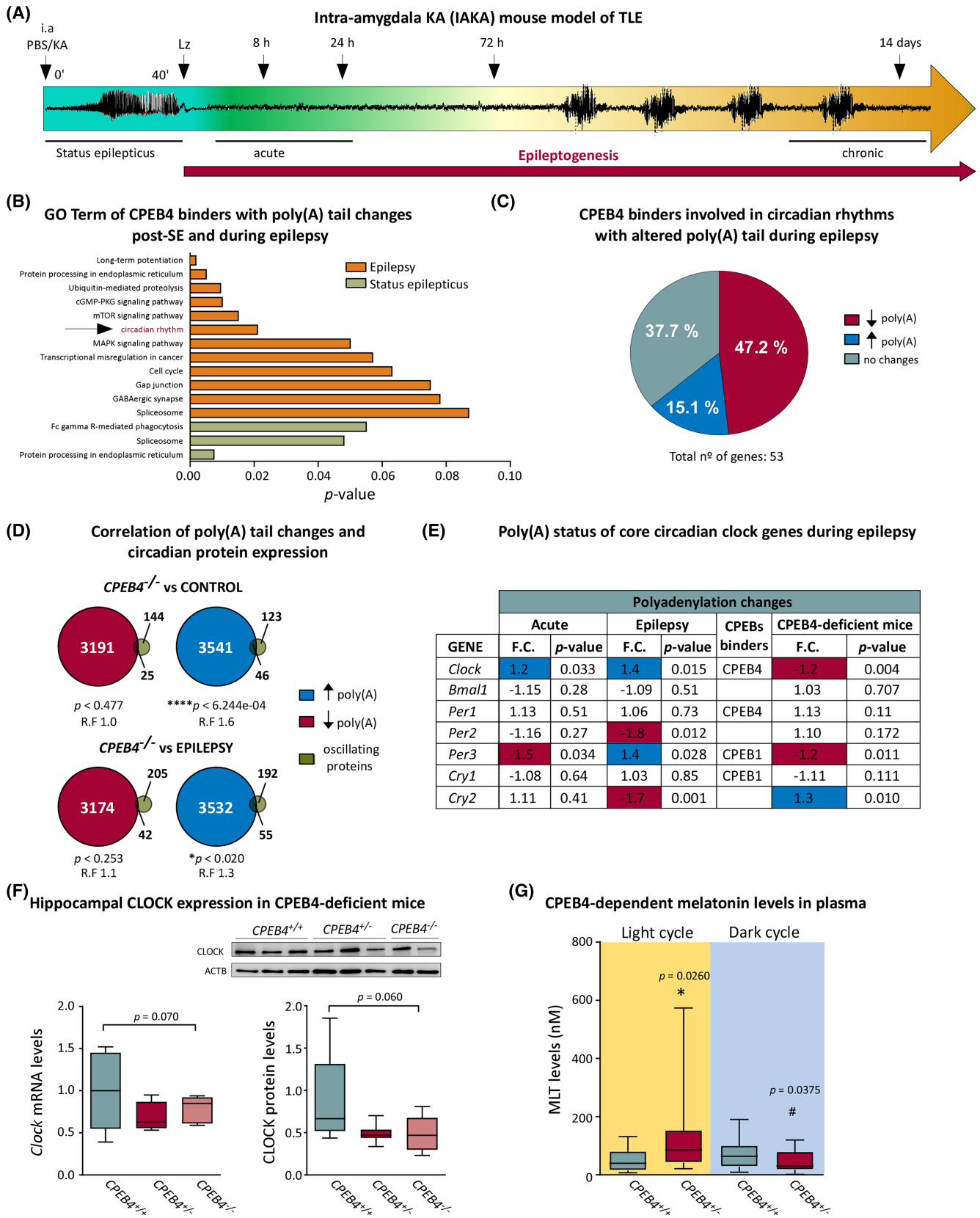


**FIGURE 1** Clock binding to the CPEB4 promoter after status epilepticus (SE). (A) Diagram showing *Clock* binding site to the wild-type (WT) sequence of the *Cpeb4* 3' untranslated region Transcriptional start site (TSS). (B) Percent of CLOCK binding input in the ipsilateral hippocampus of WT mice injected with vehicle ( $n = 18$ , three samples per pool) and kainic acid (KA) ( $n = 18$ , three samples per pool), 1 h after SE that represents the amount of chromatin used in the chromatin immunoprecipitation (ChIP) assay. IgG-negative control is shown. (C) *Clock* and *Cpeb4* transcript levels 24 h posttransfection of N2A cells with *Clock* overexpressing plasmid. Green fluorescent protein-transfected N2A cells were used as control (Ctrl;  $n = 6$  per group). (D) CPEB4 protein levels in the ipsilateral dentate gyrus of the hippocampus of WT mice treated with vehicle (Ctrl;  $n = 4$ ) or KA ( $n = 4$ ) 1 h after SE. Protein quantity was normalized to the loading control  $\beta$ -actin (ACTB). Data are mean  $\pm$  SEM with 95% confidence intervals. \* $p < .05$ , \*\*\* $p < .001$  by unpaired  $t$ -test.



among genes with an altered poly(A) tail post-SE (7.4% no change vs. 14.2% shortened and 11.5% lengthened) and during epilepsy (6% no change vs. 13.8% shortened and 10.8% lengthened; Figure S1). More specifically, 235

CPEB4 binders (1.09% of total transcriptome analyzed) changed their poly(A) tail length (shortened and lengthened) post-SE and 721 CPEB4 binders (3.34% of total transcriptome analyzed) changed their poly(A) tail length

**FIGURE 2** CPEB4-mediated mRNA polyadenylation and regulation of circadian rhythms. (A) Schematic showing the experimental design using the intraamygdala kainic acid (KA) mouse model. Mice injected with KA develop epilepsy after a short latent period of 3–5 days. Ipsilateral hippocampi were collected at 8 h (acute phase) and 14 days (chronic phase; epilepsy) after status epilepticus (SE). i.a., intra-amygdala; Lz = lorazepam; PBS, phosphate-buffered saline; TLE, temporal lobe epilepsy. (B) Top Gene Ontology (GO) terms and associated biological processes of transcripts enriched with CPEB4 binders undergoing poly(A) tail changes post-SE and during epilepsy; *p*-value is plotted on the x-axis. (C) Percentage of circadian-related transcripts (total of 53 genes) showing poly(A) tail changes and enriched with CPEB4 binders during epilepsy. (D) Venn diagram showing overlap of transcripts undergoing poly(A) tail changes in CPEB4-deficient mice versus their encoding products in experimental epilepsy. One-sided Fisher exact test was used. R.F., representation factor. (E) Table showing poly(A) tail changes of main components of the molecular clock in the ipsilateral hippocampus after SE, during epilepsy, and in CPEB4-deficient mice. Blue indicates lengthened poly(A) tail; red indicates shortened poly(A) tail. One-way analysis of variance parametric statistics with post hoc Fisher test are shown. F.C., fold change. (F) *Clock* mRNA and CLOCK protein levels in the hippocampus of naïve CPEB4-deficient mice ( $n = 5$  [*CPEB4*<sup>+/+</sup>],  $n = 4–6$  [*CPEB4*<sup>+/-</sup>], and  $n = 5$  [*CPEB4*<sup>-/-</sup>]). ACTB,  $\beta$ -actin. (G) Melatonin (MLT) concentration in plasma of naïve *CPEB4*<sup>+/+</sup> ( $n = 10–12$ ) and *CPEB4*<sup>+/-</sup> ( $n = 8–13$ ) mice during a 24-h period (\**CPEB4*<sup>+/+</sup> light cycle vs. *CPEB4*<sup>+/-</sup> light cycle; #*CPEB4*<sup>+/-</sup> light cycle vs. *CPEB4*<sup>+/-</sup> dark cycle). \*, # $p < .05$ , \*\*\*\* $p < .001$ .

(shortened and lengthened) during epilepsy (Table S3 [acute and epilepsy]).

To identify pathways affected by CPEB4-dependent mRNA polyadenylation changes, CPEB4 binders with an altered poly(A) tail length (shortened and lengthened combined) were analyzed by Gene Ontology terms.<sup>23</sup> This analysis identified three pathways post-SE (phagocytosis, spliceosome, and endoplasmic reticulum [ER]) and several pathways during epilepsy (synaptic transmission [long-term potentiation,  $\gamma$ -aminobutyric acidergic synapse], protein processing [ER, ubiquitin-mediated proteolysis], signaling pathways [mammalian target of rapamycin, cyclic guanosine monophosphate–protein kinase G, and mitogen-activated protein kinase], genes regulating gap junctions, cell cycle, spliceosome, and genes involved in the regulation of circadian rhythms; Figure 2B). Interestingly, “circadian rhythms” were identified as one of the most significantly altered pathways during epilepsy (Figure 2B and Table S4).

Next, we focused our analysis on CPEB4 binders with an altered poly(A) tail during epilepsy that have previously been shown to be implicated in circadian rhythms (<https://www.wikipathways.org/index.php/Pathway:WP3594>) and compared these to their poly(A) status in CPEB4-deficient mice (Figure 2C and Table 1). This showed that, during epilepsy, approximately 50% of analyzed genes displayed a shortened poly(A) tail, whereas 15% showed a lengthened poly(A) tail (Figure 2C and Table 1). Notably, CPEB4-deficient mice showed the opposite poly(A) tail status of genes associated with circadian rhythms when compared to poly(A) changes observed in the IAKA epilepsy model. This was most evident in genes with a lengthened poly(A) tail during epilepsy (Table 1). In contrast, among genes associated with circadian rhythms but that have not been identified as CPEB4 binders, only 18 of 136 genes (13.2%) showed a shortened poly(A) tail and 21 of 136 genes (15.4%) showed a lengthened poly(A) tail during epilepsy (Table S5).

We next compared published datasets analyzing oscillations in protein expression in the brain during the day in experimental epilepsy<sup>24</sup> versus their poly(A) status in CPEB4-deficient mice.<sup>9</sup> This revealed that genes linked to CPEB4 are enriched among proteins changing their expression according to the time of the day under both control conditions (71/169 genes; representation factor [R.F] = 1.3,  $p < .005$ ) and during epilepsy (97/247 genes; R.F = 1.2,  $p < .013$ ). Notably, although cross comparison of proteins with altered expression during the day also showed a correlation with the poly(A) profile in CPEB4-deficient mice, this was restricted to genes with a lengthened poly(A) tail (control: 46/169 genes, R.F = 1.6,  $p < .0004$ ; epilepsy: 55/247 genes, R.F = 1.3;  $p < .020$ ; Figure 2D), further in line with our results indicating that CPEB4 binders with a longer poly(A) tail in CPEB4-deficient mice and, hence, shorter poly(A) tail in our epilepsy model, are mostly affected in epilepsy.

When focusing on the main core proteins involved in the regulation of circadian rhythms, *Clock* was the only CPEB4 binder showing a lengthened poly(A) tail during SE and epilepsy and, conversely, an opposite poly(A) tail pattern in CPEB4-deficient mice (Figure 2E). In line with a shortened poly(A) tail in CPEB4-deficient mice, hippocampal CLOCK mRNA and protein expression, although not reaching significance, was slightly reduced in naïve CPEB4-deficient (*CPEB4*<sup>+/-</sup> and *CPEB4*<sup>-/-</sup>) mice (Figure 2F). Naïve CPEB4-deficient mice also showed altered mRNA levels of other components of the molecular clock such as the transcriptional activator *Bmal1* and transcriptional repressor *Cry1* (Figure S2).

We next analyzed serum melatonin levels in WT (*CPEB4*<sup>+/+</sup>) and CPEB4-deficient (*CPEB4*<sup>+/-</sup>) mice at two different timepoints, 10:00 a.m. (light cycle) and 09:00 p.m. (dark cycle), over a 24-h period in a 12-h light–dark cycle. Serum melatonin levels were slightly increased during the dark cycle in naïve WT mice (~20%; Figure 2G). More strikingly, melatonin levels in serum of *CPEB4*<sup>+/-</sup> mice

**TABLE 1** Poly(A) status of transcripts with a dynamic control of gene expression and CPEB4 binders during epilepsy.

| Gene  | Polyadenylation changes |                    |                      |                    |
|---|-------------------------|--------------------|----------------------|--------------------|
|   | Epilepsy                |                    | CPEB4-deficient mice |                    |
|   | F.C.                    | p                  | F.C.                 | p                  |
| <i>Hnrnpd</i> (heterogeneous nuclear ribonucleoprotein D)                                 | -2.45 <sup>a</sup>      | .0000 <sup>b</sup> | 1.33 <sup>c</sup>    | .0010 <sup>b</sup> |
| <i>Hdac2</i> (histone deacetylase 2)  | -2.39 <sup>a</sup>      | .0010 <sup>d</sup> | 1.11                 | .1430              |
| <i>Nono</i> (non-POU-domain-containing, octamer binding protein)                          | -2.30 <sup>a</sup>      | .0037 <sup>d</sup> | 1.28 <sup>c</sup>    | .0030 <sup>e</sup> |
| <i>Gnaq</i> (guanine nucleotide binding protein, alpha q polypeptide)                     | -2.08 <sup>a</sup>      | .0008 <sup>b</sup> | 1.30 <sup>c</sup>    | .0040 <sup>e</sup> |
| <i>Klf10</i> (Kruppel-like factor 10)   | -1.91 <sup>a</sup>      | .0119 <sup>f</sup> | 1.01                 | .9610              |
| <i>Ppargc1a</i> (peroxisome proliferative activated receptor, gamma, coactivator 1 alpha) | -1.85 <sup>a</sup>      | .0067 <sup>d</sup> | 1.20 <sup>c</sup>    | .0270 <sup>f</sup> |
| <i>Ppp1cc</i> (protein phosphatase 1, catalytic subunit, gamma isoform)                   | -1.68 <sup>a</sup>      | .0003 <sup>b</sup> | 1.06                 | .4330              |
| <i>Arnt2</i> (aryl hydrocarbon receptor nuclear translocator 2)                           | -1.63 <sup>a</sup>      | .0010 <sup>b</sup> | -1.16                | .1020              |
| <i>Skp1a</i> (S-phase kinase-associated protein 1A)                                       | -1.63 <sup>a</sup>      | .0029 <sup>d</sup> | -1.12 <sup>a</sup>   | .0490 <sup>f</sup> |
| <i>Rorb</i> (RAR-related orphan receptor beta)  | -1.56 <sup>a</sup>      | .0031 <sup>d</sup> | -1.18                | .1020              |
| <i>Egr3</i> (early growth response 3)   | -1.52 <sup>a</sup>      | .0276 <sup>f</sup> | 1.19 <sup>c</sup>    | .0150 <sup>f</sup> |
| <i>Ppp1cb</i> (protein phosphatase 1, catalytic subunit, beta isoform)                    | -1.52 <sup>a</sup>      | .0002 <sup>b</sup> | 1.34 <sup>c</sup>    | .0080 <sup>e</sup> |
| <i>Prox1</i> (prospero-related homeobox 1)  | -1.51 <sup>a</sup>      | .0020 <sup>d</sup> | 1.52 <sup>c</sup>    | .0004 <sup>b</sup> |
| <i>Rora</i> (RAR-related orphan receptor alpha)   | -1.49 <sup>a</sup>      | .0157 <sup>f</sup> | 1.00                 | 1.0                |
| <i>Dyrk1a</i> (dual-specificity tyrosine-(Y)-phosphorylation regulated kinase 1a)         | -1.47                   | .0700              | 1.27 <sup>c</sup>    | .0100 <sup>e</sup> |
| <i>Pten</i> (phosphatase and tensin homolog)  | -1.46 <sup>a</sup>      | .0199 <sup>f</sup> | 1.27 <sup>c</sup>    | .0020 <sup>d</sup> |
| <i>Klf9</i> (Kruppel-like factor 9)   | -1.46 <sup>a</sup>      | .0084 <sup>d</sup> | 1.72 <sup>c</sup>    | .0003 <sup>b</sup> |
| <i>Nampt</i> (nicotinamide phosphoribosyltransferase)                                     | -1.40 <sup>a</sup>      | .0207 <sup>f</sup> | -1.29 <sup>a</sup>   | .0030 <sup>d</sup> |
| <i>Hs3st2</i> (heparan sulfate (glucosamine) 3-O-sulfotransferase 2)                      | -1.40 <sup>a</sup>      | .0414 <sup>f</sup> | -1.40 <sup>a</sup>   | .0010 <sup>b</sup> |
| <i>Kcnd2</i> (potassium voltage-gated channel, Shal-related family, member 2)             | -1.38 <sup>a</sup>      | .0202 <sup>f</sup> | 1.30 <sup>c</sup>    | .0030 <sup>d</sup> |
| <i>Npas2</i> (neuronal PAS domain protein 2)  | -1.38 <sup>a</sup>      | .0338 <sup>f</sup> | -1.05                | .4940              |
| <i>Jun</i> (Jun oncogene)   | -1.35 <sup>a</sup>      | .0126 <sup>f</sup> | 1.25 <sup>c</sup>    | .0040 <sup>d</sup> |
| <i>Creb1</i> (cAMP responsive element binding protein 1)                                  | -1.31 <sup>a</sup>      | .0315 <sup>f</sup> | -1.36 <sup>a</sup>   | .0020 <sup>d</sup> |
| <i>Ncor1</i> (nuclear receptor corepressor 1)   | -1.30 <sup>a</sup>      | .0100 <sup>d</sup> | 1.15                 | .0530              |
| <i>Zfhlx3</i> (zinc finger homeobox 3)  | -1.28                   | .0900              | 1.20                 | .1140              |
| <i>Top1</i> (topoisomerase (DNA) I)   | -1.27 <sup>a</sup>      | .0406 <sup>f</sup> | 1.15 <sup>c</sup>    | .0400 <sup>f</sup> |
| <i>Adcy1</i> (adenylate cyclase 1)  | -1.21 <sup>a</sup>      | .0452 <sup>f</sup> | -1.16 <sup>a</sup>   | .0210 <sup>f</sup> |
| <i>Ogt</i> (UDP-N-acetylglucosamine:polypeptide-N-acetylglucosaminyl transferase)         | -1.17                   | .2100              | -1.26 <sup>a</sup>   | .0160 <sup>f</sup> |
| <i>Fbxl3</i> (F-box and leucine-rich repeat protein 3)                                    | -1.16                   | .4500              | 1.28 <sup>c</sup>    | .0087 <sup>d</sup> |
| <i>Egr1</i> (early growth response 1)   | -1.07                   | .7500              | 1.17 <sup>c</sup>    | .0210 <sup>f</sup> |
| <i>Mapk8</i> (mitogen-activated protein kinase 8)   | 1.00                    | 1.0                | 1.21 <sup>c</sup>    | .0300 <sup>f</sup> |
| <i>Nrip1</i> (nuclear receptor interacting protein 1)                                     | 1.00                    | 1.0                | 1.00                 | 1.0                |
| <i>Ntrk3</i> (neurotrophic tyrosine kinase, receptor, type 3)                             | 1.00                    | 1.0                | 1.21 <sup>c</sup>    | .0360 <sup>f</sup> |



TABLE 1 (Continued)

| Gene   | Polyadenylation changes |                    |                      |                    |
|--|-------------------------|--------------------|----------------------|--------------------|
|  | Epilepsy                |                    | CPEB4-deficient mice |                    |
|  | F.C.                    | p                  | F.C.                 | p                  |
| <i>Sfpq</i> (splicing factor proline/glutamine rich)                     | 1.00                    | 1.0                | 1.00                 | 1.0                |
| <i>Ube3a</i> (ubiquitin protein ligase E3A)                              | 1.00                    | 1.0                | 1.00                 | 1.0                |
| <i>Nlgn1</i> (neuroligin 1)  | 1.03                    | .7400              | 1.08                 | .1590              |
| <i>Per1</i> (period circadian clock 1)                                   | 1.06                    | .7300              | 1.13                 | .1090              |
| <i>Adora2a</i> (adenosine A2a receptor)                                  | 1.12                    | .1800              | -1.12                | .0680              |
| <i>Crem</i> (cAMP responsive element modulator)                          | 1.13                    | .1100              | 1.11                 | .1270              |
| <i>Nr1d2</i> (nuclear receptor subfamily 1, group D, member 2)           | 1.17                    | .1500              | -1.11                | .1240              |
| <i>Dhx9</i> (DEAH (Asp-Glu-Ala-His) box polypeptide 9)                   | 1.18                    | .0530              | 1.17                 | .0630              |
| <i>Kdm5a</i> (lysine (K)-specific demethylase 5A)                        | 1.22                    | .0800              | 1.21 <sup>c</sup>    | .0120 <sup>f</sup> |
| <i>Homer1</i> (homer homolog 1 (Drosophila))                             | 1.35                    | .0800              | 1.21 <sup>c</sup>    | .0190 <sup>f</sup> |
| <i>Pspc1</i> (paraspeckle protein 1)                                     | 1.36                    | .0800              | -1.16 <sup>a</sup>   | .0390 <sup>f</sup> |
| <i>Crh</i> (corticotropin releasing hormone)                             | 1.37                    | .4200              | -1.16                | .1020              |
| <i>Clock</i> (circadian locomotor output cycles kaput)                   | 1.41 <sup>c</sup>       | .0145 <sup>f</sup> | -1.23 <sup>a</sup>   | .0039 <sup>d</sup> |
| <i>Hdac1</i> (histone deacetylase 1)                                     | 1.43 <sup>c</sup>       | .0086 <sup>e</sup> | -1.07                | .5470              |
| <i>Dbp</i> (D site albumin promoter binding protein)                     | 1.53 <sup>c</sup>       | .0029 <sup>d</sup> | 1.26 <sup>c</sup>    | .0241 <sup>f</sup> |
| <i>Prkaa2</i> (protein kinase, AMP-activated, alpha 2 catalytic subunit) | 1.57 <sup>c</sup>       | .0063 <sup>e</sup> | 1.10                 | .4120              |
| <i>Ddx5</i> (DEAD (Asp-Glu-Ala-Asp) box polypeptide 5)                   | 1.77 <sup>c</sup>       | .0005 <sup>b</sup> | -1.21                | .1410              |
| <i>Rock2</i> (Rho-associated coiled-coil containing protein kinase 2)    | 1.82 <sup>c</sup>       | .0077 <sup>e</sup> | -1.20 <sup>a</sup>   | .0180 <sup>f</sup> |
| <i>Csnk1d</i> (casein kinase 1, delta)                                   | 2.55 <sup>c</sup>       | .0025 <sup>d</sup> | -1.13                | .1220              |
| <i>Id4</i> (inhibitor of DNA binding 4)                                  | 2.58 <sup>c</sup>       | .0015 <sup>d</sup> | 1.25 <sup>c</sup>    | .0170 <sup>f</sup> |

Abbreviation: F.C., fold change.

<sup>a</sup>Shortened poly(A) tail.

<sup>b</sup> $p < .001$ .

<sup>c</sup>Lengthened poly(A) tail.

<sup>d</sup> $p < .005$ .

<sup>e</sup> $p < .01$ .

<sup>f</sup> $p < .05$ .

showed the reverse, with higher levels observed during the light cycle and lower levels during the dark cycle (~50%). Moreover, melatonin levels were higher during the day cycle and lower during the night cycle when compared to WT mice (Figure 2G).

### 3.3 | Increased CLOCK expression in the hippocampus of mice following SE and in patients with TLE

To validate our microarray data and test whether a lengthened poly(A) tail found in *Clock* transcripts post-SE and during epilepsy is translated into an increase in CLOCK protein expression, we analyzed hippocampal tissue from

WT mice subjected to IAKA shortly following SE and during epilepsy. Hippocampal *Clock* mRNA levels were increased 8 and 24 h post-SE (Figure 3A), and CLOCK protein expression was increased 24 h post-SE (Figure 3B). A similar increase was observed during epilepsy (i.e., 14 days post-SE), where *Clock* mRNA levels were slightly upregulated in the hippocampus (Figure 3C) and CLOCK protein levels increased (Figure 3D). In addition, we analyzed expression changes of other components of the molecular clock, including BMAL1, CRY1, and PER2, post-SE and during epilepsy. Whereas the expression of BMAL1 and PER2 was increased post-SE, no changes were observed for CRY1 (Figure S3A). During epilepsy, BMAL1 levels were decreased, and no changes were observed for CRY1 and PER2 (Figure S3B).

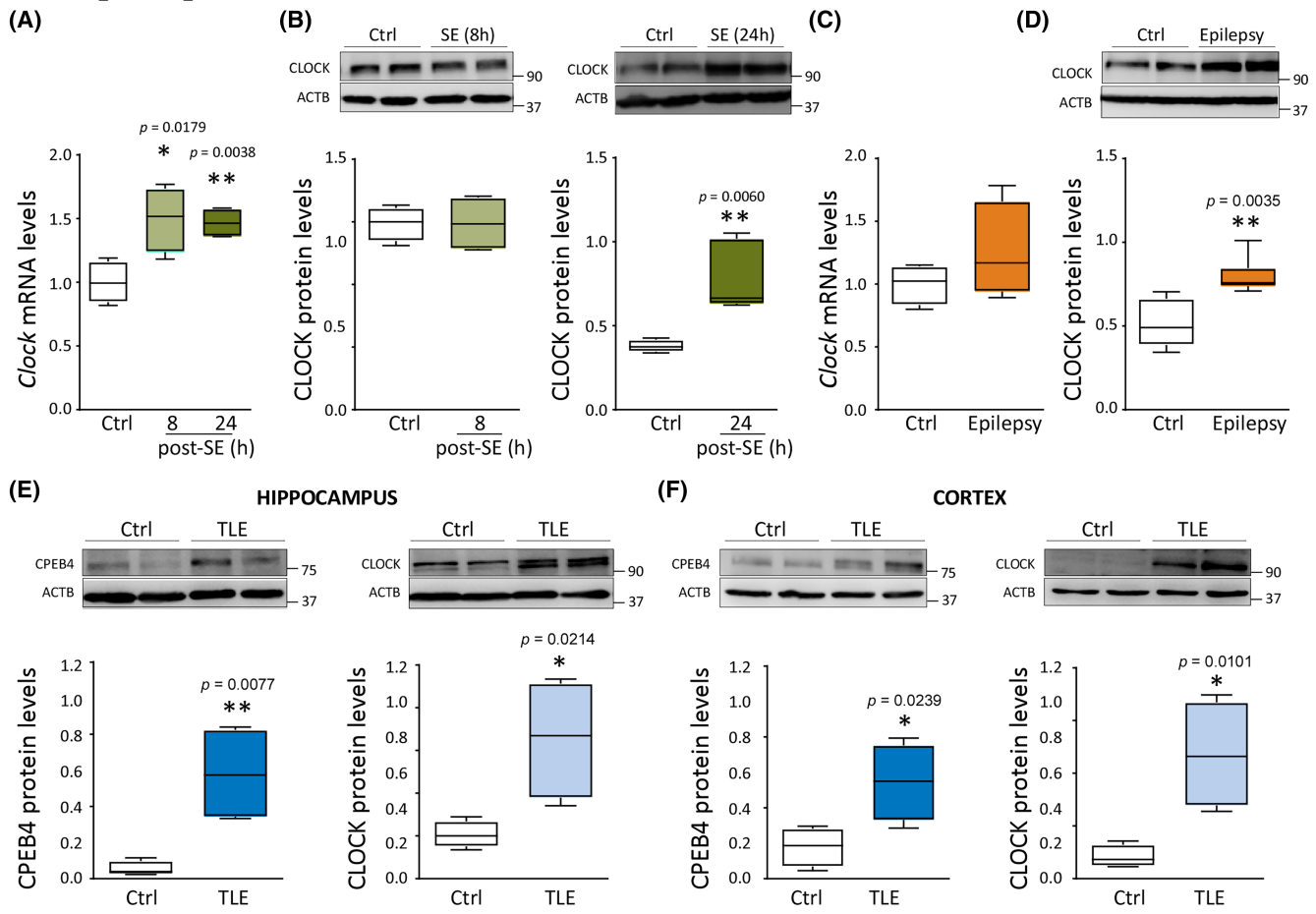


**FIGURE 3** Clock protein expression in the brain following status epilepticus (SE) and during epilepsy in mice and in temporal lobe epilepsy (TLE) patients. (A) *Clock* mRNA and (B) CLOCK protein levels in the ipsilateral hippocampus of wild-type (WT) mice injected with vehicle (Ctrl,  $n = 4$ ) and kainic acid (KA; SE,  $n = 4$ ) at 8h and 24h post-SE. (C) *Clock* mRNA and (D) CLOCK protein levels in the ipsilateral hippocampus of WT mice injected with vehicle (Ctrl,  $n = 4$ ) and KA (SE,  $n = 4$ ) at 14 days after SE. (E) Hippocampal and (F) cortical CPEB4 and CLOCK protein levels of patients with TLE and control ( $n = 4$  per group). Protein quantity was normalized to the loading control  $\beta$ -actin (ACTB). Data are mean  $\pm$  SEM with 95% confidence intervals. \* $p < .05$ , \*\* $p < .01$  by unpaired  $t$ -test.

We next analyzed resected cortical and hippocampal tissue obtained after resection surgery from drug-refractory TLE patients. In line with what we had reported previously, CPEB4 protein levels were highly increased in the hippocampus<sup>11</sup> and cortex (Figure 3E,F). Likewise, CLOCK protein levels were also increased in hippocampal and cortical tissue by approximately twofold (Figure 3E,F).

### 3.4 | CPEB4-deficient mice present decreased CLOCK expression post-SE in the hippocampus and an altered circadian seizure phenotype

We then investigated the impact of CPEB4-deficiency on CLOCK expression after SE. CPEB4-deficient mice displayed a decrease in hippocampal CLOCK protein levels at both 8 and 24h post-SE (Figure 4A), further suggesting CLOCK expression to be under the control of CPEB4.

Finally, to determine whether the deletion of *Cpeb4* has an impact on the seizure rhythmicity, we analyzed the seizure phenotype of epileptic WT (*CPEB4*<sup>+/+</sup>) and CPEB4-deficient (*CPEB4*<sup>+/-</sup>) mice. Interestingly, *CPEB4*<sup>+/-</sup> mice showed an opposite pattern in the number of seizures experienced along the day compared to WT mice, experiencing more seizures during the dark cycle when compared to the light cycle (Figure 4B).

## 4 | DISCUSSION

Posttranscriptional regulatory mechanisms are widely recognized to contribute to epilepsy development.<sup>1-3</sup> Among these, mRNA polyadenylation has only recently emerged as a new player in epileptogenesis.<sup>11</sup> Moreover, CPEB4 has been identified as a major contributor to these changes.<sup>11</sup> Although there is growing evidence of CPEB4 contributing to several brain pathologies,<sup>5</sup> what drives

CPEB4 expression during brain diseases has not been analyzed to date.

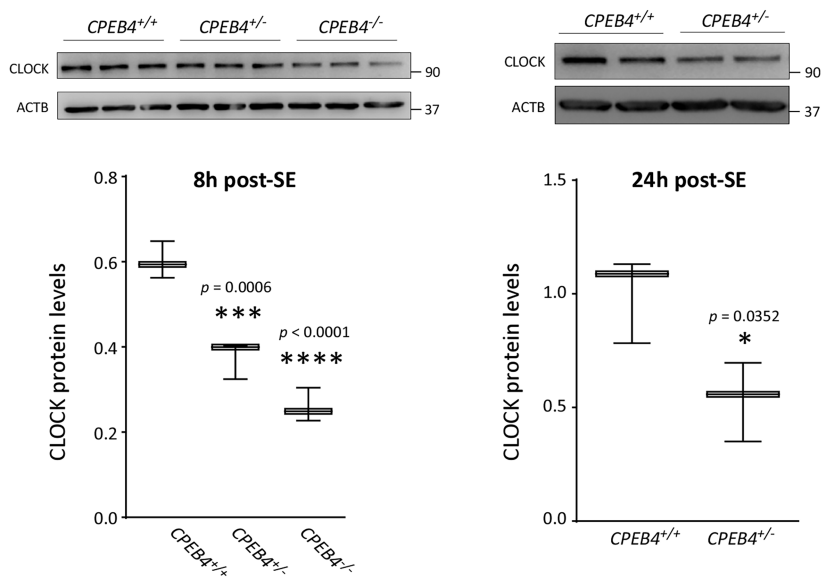
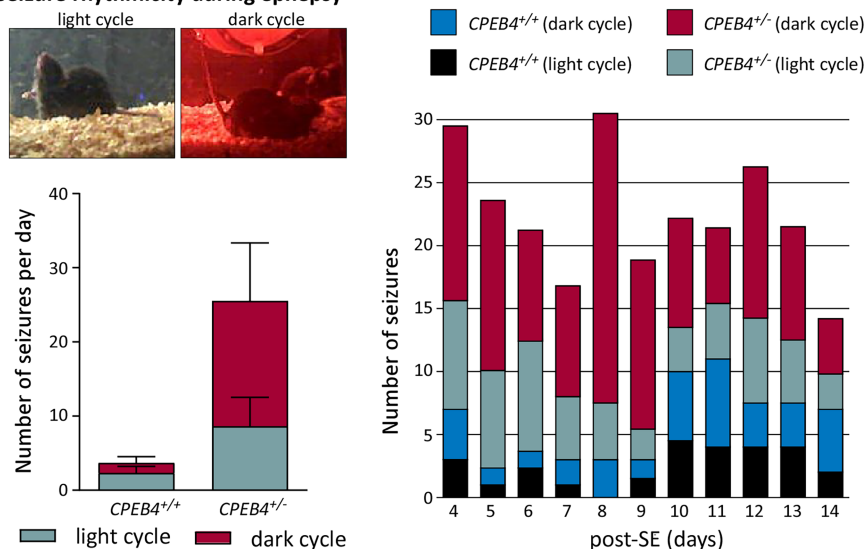
Our first finding shows that CLOCK binds to the promoter region of *Cpeb4* during the physiological condition, which increases post-SE. We also show that overexpression of CLOCK leads to increased *Cpeb4* transcript levels. CPEB4 expression has previously been shown to oscillate in a 24-h fashion in hepatic tissue.<sup>16,17</sup> Hence, it is tempting to speculate that circadian expression changes of CPEB4 are, at least in part, regulated via CLOCK. Definite proof of CLOCK regulating the circadian expression of CPEB4 would, however, require the analyses of cyclic CPEB4 expression in CLOCK-deficient mice.

Here, we show that the total number of identified CPEB4-dependent pathways is higher during epilepsy when compared to SE. This is, however, most likely simply a direct consequence of poly(A) changes being much more pronounced during epilepsy.<sup>11</sup> Although circadian rhythms were one of the top pathways identified during epilepsy, our analysis identified several other pathways potentially under the control of CPEB4. Of note, ER stress, identified during both SE and epilepsy, has a known role during epilepsy development<sup>25</sup> and has previously been shown to be regulated via CPEB4 in the liver.<sup>17</sup>

It is increasingly clear that changes in the sleep–wake cycle contribute to epilepsy development. Sleep deprivation is a known trigger of seizures.<sup>12,26</sup> Both CLOCK and BMAL1 deficiency have been reported to lower the seizure threshold in rodents.<sup>13,14</sup> This not only demonstrates a role of core clock proteins during seizure generation and epilepsy development, but also suggests that increasing CLOCK protein expression in the brain may represent a protective mechanism against seizures. Of note, CPEB4-deficient mice show lower CLOCK brain levels, potentially contributing to their increased brain hyperexcitability.<sup>11</sup> We have previously shown that a shorter poly(A) tail leads to a decrease in protein expression in the brain<sup>9,11</sup>; hence, we can speculate that a longer poly(A) tail observed in *Clock* leads to the observed increase in its expression, most likely regulated via CPEB4. Why, in contrast to the lower CLOCK brain levels reported in other studies,<sup>14,27</sup> CLOCK was increased post-IACA and in TLE patient brain, remains to be determined. Possible explanations include the use of different models and species or timepoints during disease progression at which samples were analyzed. We have, however, shown that the IACA model closely mimics the human condition at the molecular level,<sup>28</sup> and we have obtained similar results in our mouse model and patients. Nevertheless, the effects of CPEB4 on epilepsy being restricted to its impact on the regulation of circadian rhythms is unlikely; most likely, several pathways are affected simultaneously.

In addition, our results show that the expression of other molecular components of the core clock proteins is altered in brain tissue of CPEB4-deficient mice. Although this may be a consequence of CPEB4 targeting CLOCK, this further demonstrates the critical role CPEB4 plays in the regulation of circadian rhythms in the brain. Alterations in circadian rhythms in CPEB4-deficient mice are further evidenced by altered melatonin levels in their blood. Melatonin is the primary hormone integrating sleep–wake cycle and circadian rhythms.<sup>29</sup> Moreover, treatment of epileptic rodents and patients with melatonin has shown anticonvulsive effects.<sup>30–32</sup> This seems, however, to be dependent on melatonin concentrations, with too high melatonin concentrations also having proconvulsive effects.<sup>33</sup> In patients, despite showing normal rhythmicity, melatonin levels have been reported to be lower when compared to control.<sup>34</sup> Our results showed opposing plasma melatonin levels in CPEB4-deficient mice when compared to WT mice, with melatonin levels being higher during the night and lower during the day, suggesting a shift in circadian plasma melatonin levels in CPEB4-deficient mice throughout the day. Of note, CPEB4-deficient mice also experienced more epileptic seizures during the night, possibly as a consequence of increased melatonin blood levels. However, regardless, whether the higher seizure susceptibility observed in CPEB4-deficient mice is due to altered melatonin concentrations or whether altered melatonin levels are a consequence of altered expression of core clock proteins in CPEB4-deficient mice, our results are the first to report CPEB4-mediated mRNA polyadenylation in the brain as a new contributor to the regulation of the sleep–wake cycle.

Transcription-translation feedback loops (TTFLs) are an essential mechanism to generate and sustain approximately 24-h rhythms in cells.<sup>35</sup> In mammals, the primary TTFL involves interactions between transcriptional activators (e.g., BMAL1, CLOCK) and the repressive complex formed by, for example, PER and CRY. TTFL are, however, much more complex and are further regulated by secondary feedback loops to further fine-tune protein expression and protein expression oscillations.<sup>36</sup> Circadian transcription may be further impacted by different transcription factors, chromatin remodeling, and posttranscriptional changes such as mRNA polyadenylation.<sup>16</sup> Studies in liver tissue have shown a strong correlation between poly(A) tail length rhythmicity and protein rhythms, where the peak tail length precedes the peak in protein expression. These were, at least in some cases, regulated via CPEBs.<sup>16</sup> We here describe a new TTFL involving CLOCK and CPEB4, representing a possible amplification loop for both CPEB4 and CLOCK, thereby fine-tuning the expression of hundreds of mRNAs and impacting on a plethora of intracellular pathways.

**(A) Hippocampal CLOCK expression in CPEB4-deficient mice post-SE****(B) Seizure rhythmicity during epilepsy**

**FIGURE 4** CPEB4-deficient mice present decreased CLOCK expression in the hippocampus and an altered sleep–wake cycle. (A) Protein levels of CLOCK in the ipsilateral hippocampus of CPEB4-deficient mice at 8 h and 24 h after status epilepticus (SE;  $n = 3$  [*CPEB4*<sup>+/+</sup>],  $n = 3$  [*CPEB4*<sup>+/-</sup>],  $n = 3$  [*CPEB4*<sup>-/-</sup>]). Protein quantity was normalized to the loading control  $\beta$ -actin (ACTB). (B) Top left panel: Photographs showing mice displaying spontaneous seizures during the dark and light cycles. Bottom left panel: Average of daily spontaneous seizures in *CPEB4*<sup>+/+</sup> ( $n = 3$ ) and *CPEB4*<sup>+/-</sup> ( $n = 8$ ) mice in 24-h period during 14-day recording period (starting at the time of intra-amygdala kainic acid treatment). Right panel: Graph showing daily seizure frequency according to time of day. Data are mean  $\pm$  SEM with 95% confidence intervals. \* $p < .05$ , \*\*\* $p < .001$ , \*\*\*\* $p < .0001$  by unpaired  $t$ -test.

A possible limitation of our study is that our research focused specifically on CPEB4; other CPEBs and other RNA binding proteins are, however, most likely also implicated not only in mediating poly(A) tail length changes during epilepsy but also in the regulation of the sleep–wake cycle. In our study, we have restricted tissue analysis to one timepoint of the day (i.e., morning). Therefore, the analysis of several timepoints during the day should be carried out in future studies. In addition, different cell type compositions between control and patient brain may impact on gene expression levels. Also, although we have shown increased CLOCK and CPEB4 expression in cortical and hippocampal tissue in TLE patients, we cannot exclude postmortem effects in control samples contributing to the observed differences. Moreover, our analysis was

restricted to male mice. Sex differences in behavioral circadian rhythms in rodents have, however, been reported previously.<sup>37</sup> In this context, it is, however, worth pointing out that in our previous study both male and female CPEB4-deficient mice experienced more severe seizures during SE when compared to WT mice.<sup>11</sup> Finally, our analysis was restricted to the IAKA mouse model. Our findings should, therefore, be replicated in other models of epilepsy in the future (e.g., TBI model, genetic epilepsies).

Taken together, our data identify a new positive transcriptional–translational feedback loop in the brain between CPEB4 and CLOCK. Consequently, CPEB4 may represent a new target gene in conditions where alterations in the sleep–wake cycle are one of the underlying pathologies.

## AUTHOR CONTRIBUTIONS

Conceptualization and methodology: Laura de Diego-Garcia, Gary P. Brennan, Aida Menendez-Mendez, Alberto Parras, Alba Martin-Gil, Theresa Auer, Meghma Mitra, Ivana Olla - Validation, formal analysis, investigation, and data curation, Leticia Villalba-Benito, Beatriz Gil, Mariana Alves, Kelvin Lau, Gonzalo Carracedo-Rodríguez, and Tobias Engel. Validation, formal analysis, investigation, and data curation: Laura de Diego-Garcia, Gary P. Brennan, Aida Menendez-Mendez, Alberto Parras, Alba Martin-Gil, Theresa Auer, Leticia Villalba-Benito, Beatriz Gil, Mariana Alves, Kelvin Lau, and Tobias Engel. Resources: Norman Delanty, Alan Beausang, Jane Cryan, Francesca M. Brett, Michael A. Farrell, Donncha F. O'Brien, Gonzalo Carracedo-Rodríguez, and Tobias Engel. Writing—original draft preparation: Laura de Diego-Garcia, José J. Lucas, and Tobias Engel. Writing—review and editing: Laura de Diego-Garcia, Raúl Mendez, David C. Henshall, Laura de Diego-Garcia, José J. Lucas, and Tobias Engel. Preparation of figures: Laura de Diego-Garcia, Gary P. Brennan, José J. Lucas, and Tobias Engel. Project administration: Tobias Engel. Funding acquisition: Laura de Diego-Garcia, Gonzalo Carracedo-Rodríguez, David C. Henshall, José J. Lucas, and Tobias Engel. All authors reviewed the manuscript.

## ACKNOWLEDGMENTS

This work was supported by funding from Science Foundation Ireland (17/CDA/4708 and cofunded under the European Regional Development Fund and by FutureNeuro industry partners 16/RC/3948); from the H2020 Marie Skłodowska-Curie Actions Individual Fellowship (796600), from the Irish Research Council Postdoctoral Fellowship (GOIPD/2020/806) from the European Union's Horizon 2020 research and innovation program under the Marie Skłodowska-Curie grant agreement (No. 766124), from the Programa de Atracción de Talento de la Comunidad de Madrid (2020-T2/BMD-20180), and from the Spanish Ministry of Economy and Competitiveness/Ministry of Science, Innovation, and Universities to J.J.L. (PID2021-123141OB-I00; MCIU/AEI/FEDER,UE).

## CONFLICT OF INTEREST STATEMENT

None of the authors has any conflict of interest to disclose.

## ORCID

Laura de Diego-Garcia  <https://orcid.org/0000-0002-1404-5803>

Norman Delanty  <https://orcid.org/0000-0002-3953-9842>

David C. Henshall  <https://orcid.org/0000-0001-6237-9632>

Tobias Engel  <https://orcid.org/0000-0001-9137-0637>

## REFERENCES

- Henshall DC, Hamer HM, Pasterkamp RJ, Goldstein DB, Kjemis J, Prehn JHM, et al. MicroRNAs in epilepsy: pathophysiology and clinical utility. *Lancet Neurol*. 2016;15(13):1368–76.
- Engel T, Martinez-Villarreal J, Henke C, Jimenez-Mateos EM, Sanz-Rodriguez A, Alves M, et al. Spatiotemporal progression of ubiquitin-proteasome system inhibition after status epilepticus suggests protective adaptation against hippocampal injury. *Mol Neurodegener*. 2017;12(1):21.
- Sossin WS, Costa-Mattioli M. Translational control in the brain in health and disease. *Cold Spring Harb Perspect Biol*. 2019;11(8):a032912.
- Ivshina M, Lasko P, Richter JD. Cytoplasmic polyadenylation element binding proteins in development, health, and disease. *Annu Rev Cell Dev Biol*. 2014;30:393–415.
- Kozlov E, Shidlovskii YV, Gilmutdinov R, Schedl P, Zhukova M. The role of CPEB family proteins in the nervous system function in the norm and pathology. *Cell Biosci*. 2021;11(1):64.
- Richter JD. CPEB: a life in translation. *Trends Biochem Sci*. 2007;32(6):279–85.
- Darnell JC, Richter JD. Cytoplasmic RNA-binding proteins and the control of complex brain function. *Cold Spring Harb Perspect Biol*. 2012;4(8):a012344.
- Tseng CS, Chao HW, Huang HS, Huang YS. Olfactory-experience- and developmental-stage-dependent control of CPEB4 regulates c-Fos mRNA translation for granule cell survival. *Cell Rep*. 2017;21(8):2264–76.
- Parras A, Anta H, Santos-Galindo M, Swarup V, Elorza A, Nieto-Gonzalez JL, et al. Autism-like phenotype and risk gene mRNA deadenylation by CPEB4 mis-splicing. *Nature*. 2018;560(7719):441–6.
- Pico S, Parras A, Santos-Galindo M, Pose-Utrilla J, Castro M, Fraga E, et al. CPEB alteration and aberrant transcriptome-polyadenylation lead to a treatable SLC19A3 deficiency in Huntington's disease. *Sci Transl Med*. 2021;13(613):eabe7104.
- Parras A, de Diego-Garcia L, Alves M, Beamer E, Conte G, Jimenez-Mateos EM, et al. Polyadenylation of mRNA as a novel regulatory mechanism of gene expression in temporal lobe epilepsy. *Brain*. 2020;143:2139–53.
- Jin B, Aung T, Geng Y, Wang S. Epilepsy and its interaction with sleep and circadian rhythm. *Front Neurol*. 2020;11:327.
- Gerstner JR, Smith GG, Lenz O, Perron IJ, Buono RJ, Ferraro TN. BMAL1 controls the diurnal rhythm and set point for electrical seizure threshold in mice. *Front Syst Neurosci*. 2014;8:121.
- Li P, Fu X, Smith NA, Ziobro J, Curiel J, Tenga MJ, et al. Loss of CLOCK results in dysfunction of brain circuits underlying focal epilepsy. *Neuron*. 2017;96(2):387–401 e6.
- Wu H, Liu Y, Liu L, Meng Q, Du C, Li K, et al. Decreased expression of the clock gene Bmal1 is involved in the pathogenesis of temporal lobe epilepsy. *Mol Brain*. 2021;14(1):113.
- Kojima S, Sher-Chen EL, Green CB. Circadian control of mRNA polyadenylation dynamics regulates rhythmic protein expression. *Genes Dev*. 2012;26(24):2724–36.
- Maillo C, Martin J, Sebastian D, Hernandez-Alvarez M, Garcia-Rocha M, Reina O, et al. Circadian- and UPR-dependent control of CPEB4 mediates a translational response to counteract hepatic steatosis under ER stress. *Nat Cell Biol*. 2017;19(2):94–105.
- Calderone V, Gallego J, Fernandez-Miranda G, Garcia-Pras E, Maillo C, Berzigotti A, et al. Sequential functions of CPEB1

- and CPEB4 regulate pathologic expression of vascular endothelial growth factor and angiogenesis in chronic liver disease. *Gastroenterology*. 2016;150(4):982–97 e30.
19. Alkozi HA, Pintor J. TRPV4 activation triggers the release of melatonin from human non-pigmented ciliary epithelial cells. *Exp Eye Res*. 2015;136:34–7.
  20. Engel T, Brennan GP, Sanz-Rodriguez A, Alves M, Beamer E, Watters O, et al. A calcium-sensitive feed-forward loop regulating the expression of the ATP-gated purinergic P2X7 receptor via specificity protein 1 and microRNA–22. *Biochim Biophys Acta Mol Cell Res*. 2017;1864(2):255–66.
  21. Baud MO, Ghestem A, Benoliel JJ, Becker C, Bernard C. Endogenous multidien rhythm of epilepsy in rats. *Exp Neurol*. 2019;315:82–7.
  22. Bernard C. Circadian/multidien molecular oscillations and rhythmicity of epilepsy (MORE). *Epilepsia*. 2021;62(Suppl 1):S49–S68.
  23. Huang da W, Sherman BT, Lempicki RA. Systematic and integrative analysis of large gene lists using DAVID bioinformatics resources. *Nat Protoc*. 2009;4(1):44–57.
  24. Debski KJ, Ceglia N, Ghestem A, Ivanov AI, Brancati GE, Broer S, et al. The circadian dynamics of the hippocampal transcriptome and proteome is altered in experimental temporal lobe epilepsy. *Sci Adv*. 2020;6(41):eaat5979.
  25. Fu J, Tao T, Li Z, Chen Y, Li J, Peng L. The roles of ER stress in epilepsy: molecular mechanisms and therapeutic implications. *Biomed Pharmacother*. 2020;131:110658.
  26. Re CJ, Batterman AI, Gerstner JR, Buono RJ, Ferraro TN. The molecular genetic interaction between circadian rhythms and susceptibility to seizures and epilepsy. *Front Neurol*. 2020;11:520.
  27. Matos HC, Koike BDV, Pereira WDS, de Andrade TG, Castro OW, Duzzioni M, et al. Rhythms of Core clock genes and spontaneous locomotor activity in post-status epilepticus model of mesial temporal lobe epilepsy. *Front Neurol*. 2018;9:632.
  28. Conte G, Menendez-Mendez A, Bauer S, El-Naggar H, Alves M, Nicke A, et al. Circulating P2X7 receptor signaling components as diagnostic biomarkers for temporal lobe epilepsy. *Cell*. 2021;10(9): 2444.
  29. Hablitz LM, Molzof HE, Abrahamsson KE, Cooper JM, Prosser RA, Gamble KL. GIRK channels mediate the nonphotic effects of exogenous melatonin. *J Neurosci*. 2015;35(45):14957–65.
  30. Goldberg-Stern H, Oren H, Peled N, Garty BZ. Effect of melatonin on seizure frequency in intractable epilepsy: a pilot study. *J Child Neurol*. 2012;27(12):1524–8.
  31. Petkova Z, Tchekalarova J, Pechlivanova D, Moyanova S, Kortenska L, Mitreva R, et al. Treatment with melatonin after status epilepticus attenuates seizure activity and neuronal damage but does not prevent the disturbance in diurnal rhythms and behavioral alterations in spontaneously hypertensive rats in kainate model of temporal lobe epilepsy. *Epilepsy Behav*. 2014;31:198–208.
  32. Maghbooli M, Alyan NajafAbadi S, MalekMahmoudi G, Molseghi MH. Effect of add-on melatonin on seizure outcomes and quality of sleep in epilepsy with idiopathic generalized tonic-clonic seizures alone in adult patients: cross-sectional, randomized, double-blind, placebo-controlled clinical trial. *Brain Behav*. 2023;13:e2860.
  33. Banach M, Gurdziel E, Jedrych M, Borowicz KK. Melatonin in experimental seizures and epilepsy. *Pharmacol Rep*. 2011;63(1):1–11.
  34. Yalyn O, Arman F, Erdogan F, Kula M. A comparison of the circadian rhythms and the levels of melatonin in patients with diurnal and nocturnal complex partial seizures. *Epilepsy Behav*. 2006;8(3):542–6.
  35. Mendoza-Viveros L, Bouchard-Cannon P, Hegazi S, Cheng AH, Pastore S, Cheng HM. Molecular modulators of the circadian clock: lessons from flies and mice. *Cell Mol Life Sci*. 2017;74(6):1035–59.
  36. Lowrey PL, Takahashi JS. Genetics of circadian rhythms in mammalian model organisms. *Adv Genet*. 2011;74:175–230.
  37. Krizo JA, Mintz EM. Sex differences in behavioral circadian rhythms in laboratory rodents. *Front Endocrinol*. 2014;5:234.

## SUPPORTING INFORMATION

Additional supporting information can be found online in the Supporting Information section at the end of this article.

**How to cite this article:** de Diego-Garcia L, Brennan GP, Auer T, Menendez-Mendez A, Parras A, Martin-Gil A, et al. CPEB4–CLOCK crosstalk during temporal lobe epilepsy. *Epilepsia*. 2023;64:2827–2840. <https://doi.org/10.1111/epi.17736>